

Supplementary Material

SERCA2a stimulation by istaroxime improves intracellular Ca²⁺ handling and diastolic dysfunction in a model of diabetic cardiomyopathy

Eleonora Torre¹, Martina Arici¹, Alessandra Maria Lodrini¹, Mara Ferrandi², Paolo Barassi², Shih-Che Hsu³, Gwo-Jyh Chang⁴, Elisabetta Boz⁵, Emanuela Sala¹, Sara Vagni¹, Claudia Altomare⁶, Gaspare Mostacciuolo¹, Claudio Bussadori⁵, Patrizia Ferrari², Giuseppe Bianchi², Marcella Rocchetti¹.

Short title: SERCA2a stimulation by istaroxime in STZ-treated rats

¹Department of Biotechnology and Biosciences, Università degli Studi di Milano-Bicocca, Milan, Italy.

²Windtree Therapeutics Inc., Warrington, Pennsylvania, USA.

³CVie Therapeutics Limited, Taipei, Taiwan.

⁴Chang Gung University, Tao-Yuan, Taiwan.

⁵Clinica Veterinaria Gran Sasso, Milano, Italy.

⁶Fondazione Cardiocentro Ticino, Lugano, Switzerland.

Address for correspondence:

Marcella Rocchetti, PhD
University of Milano Bicocca
Dept. of Biotechnologies and Biosciences
P.za della Scienza, 2
20126 Milano, Italy
+39 0264483313
marcella.rocchetti@unimib.it

Supplementary figures

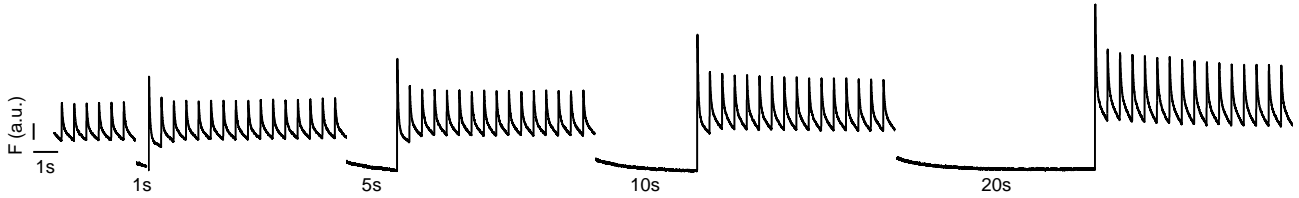


Figure S1. Post-rest potentiation protocol to evaluate SR Ca^{2+} compartmentalization during rest intervals. Field stimulated Ca^{2+} transients (Ca_T) were evocated at 2 Hz and steady state Ca_T were interrupted by increasing resting pauses (1-5-10-20 s). The amplitude of 1st Ca_T evocated following each resting pause was then normalized to the amplitude of the pre-pause ss Ca_T (see main text Fig 2).

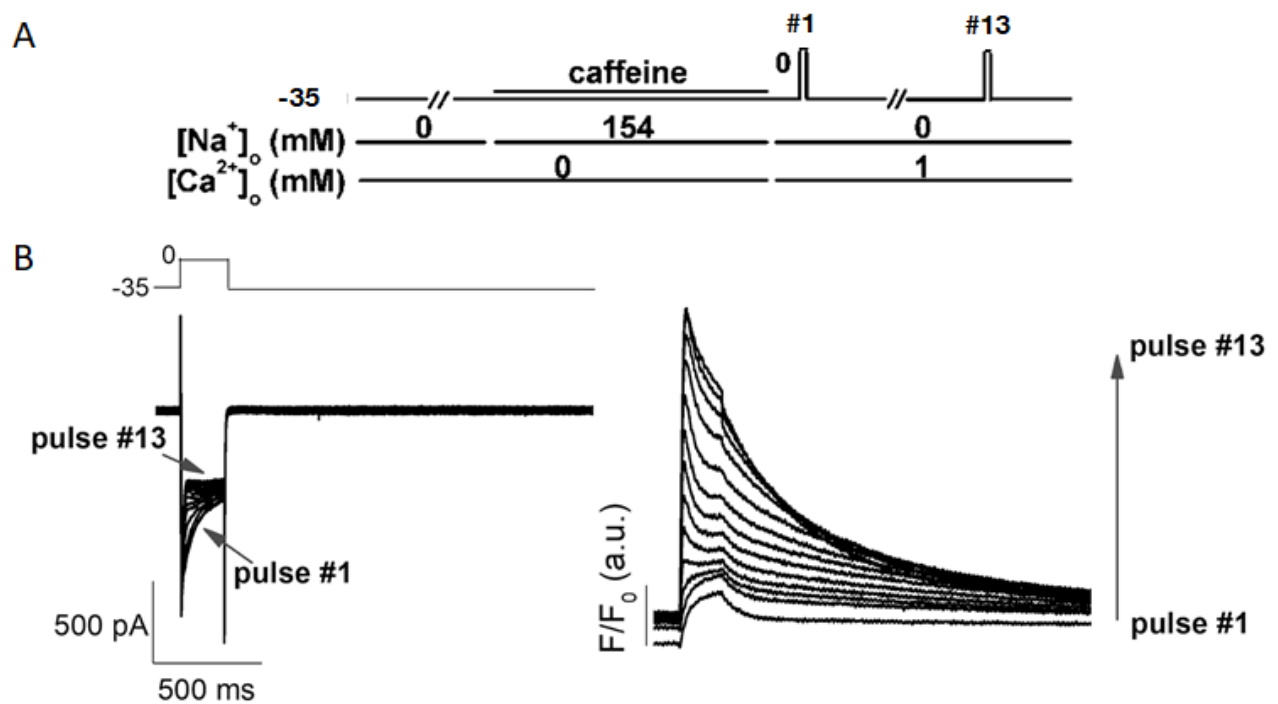


Figure S2. Protocol to evaluate Ca^{2+}_i dynamics in patch-clamped cells under Na^+ free condition. (A) Protocol outline. (B) Transmembrane current (left) and Ca^{2+} transients (right) during SR reloading after caffeine-induced SR depletion in patch-clamped cells; for details see previous work¹ and supplementary Methods below.

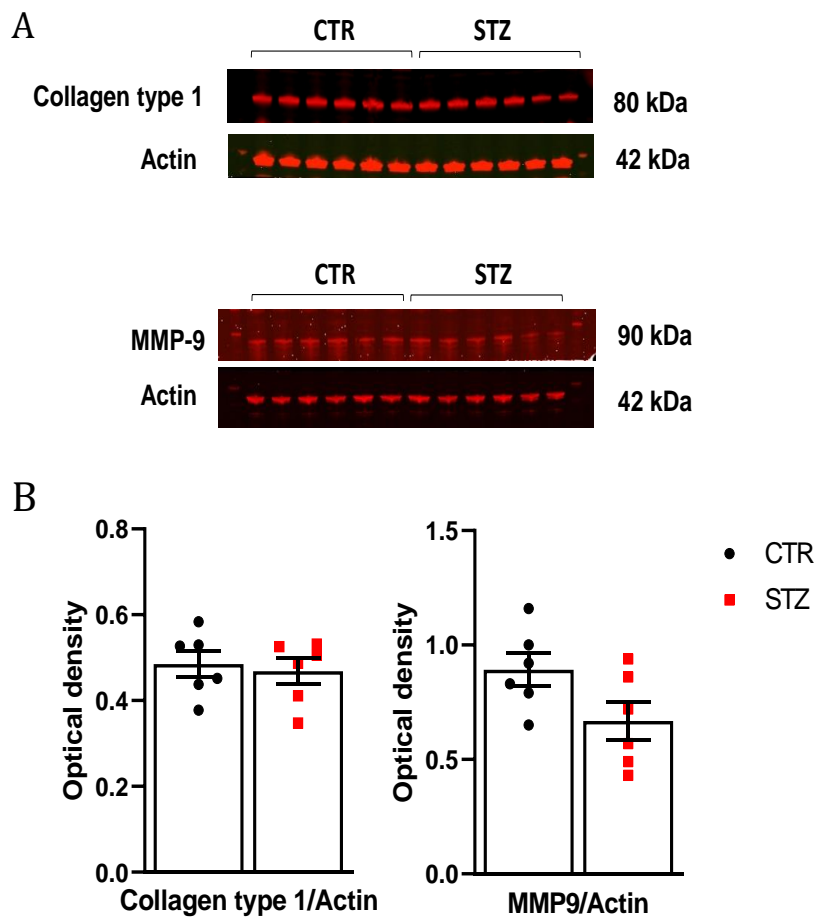


Figure S3. Protein expression levels of Collagen and MMP-9 in cardiac homogenates from CTR and STZ rats. (A) Representative Western blots for collagen type 1, matrix metalloproteinase 9 (MMP-9) and corresponding actin in cardiac homogenates from CTR and STZ rats. (B) Average results expressed as optical density in arbitrary units. CTR N=6, STZ N=6 (unpaired *t*-test).

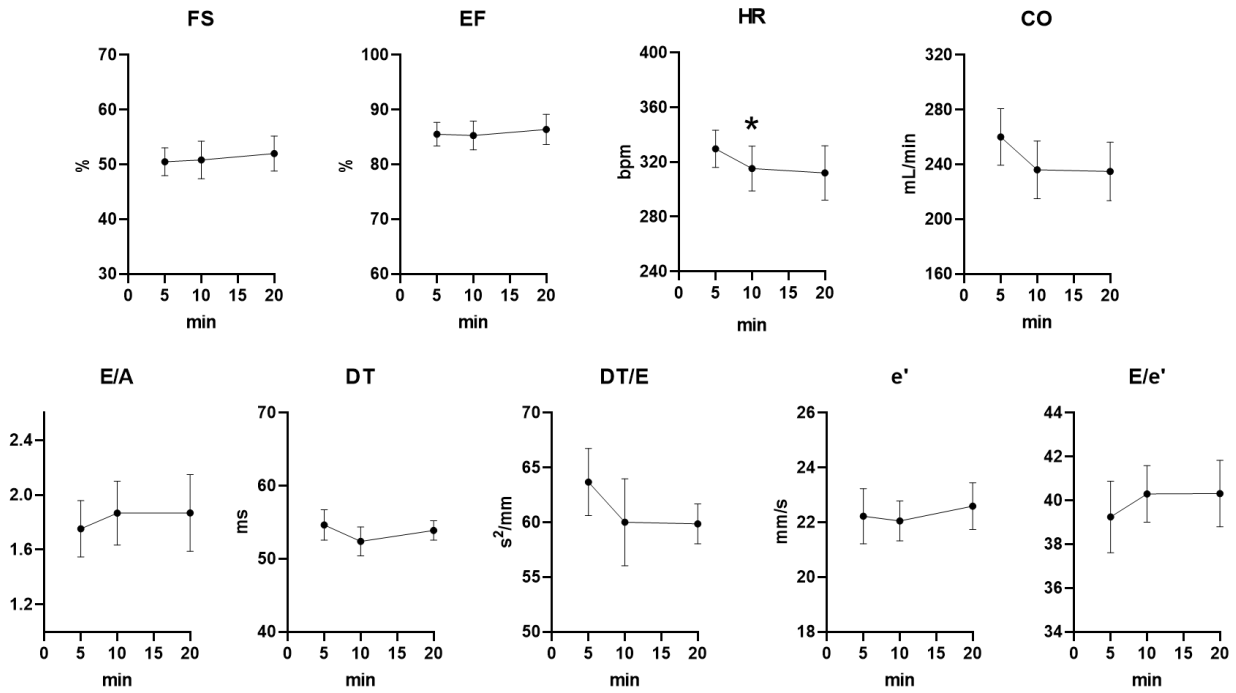


Figure S4. Time-dependent changes of echocardiographic parameters during urethane anesthesia in CTR rats. Fractional shortening (FS), ejection fraction (EF), heart rate (HR), cardiac output (CO), early (E, e') and late (A) diastolic peak velocity, deceleration time (DT). N=8. * $p < 0.05$ vs 5 min (one way ANOVA).

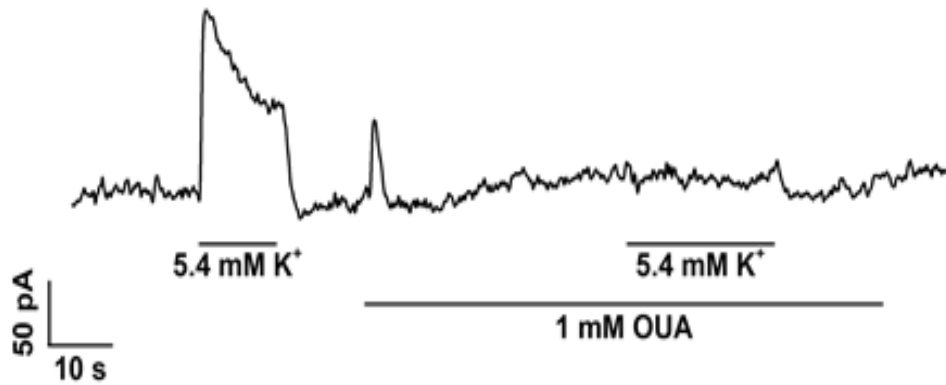


Figure S5. Saturating concentration of ouabain to block NKA in CTR rat LV cardiomyocytes. Example of membrane current recorded at -40 mV in the presence of Ni^{2+} (5 mM), nifedipine (5 μM), Ba^{2+} (1 mM) and 4-aminopyridine (2 mM) to block $\text{Na}^+/\text{Ca}^{2+}$ exchanger, Ca^{2+} and K^+ currents, respectively. Switching from extracellular K^+ free to 5.4 mM K^+ solution, activated an outward current abolished by 1 mM ouabain (OUA) pretreatment, demonstrating that the protocol is suitable to record I_{NKA} and that 1 mM OUA is a saturating concentration to block NKA in rat ventricular myocytes.

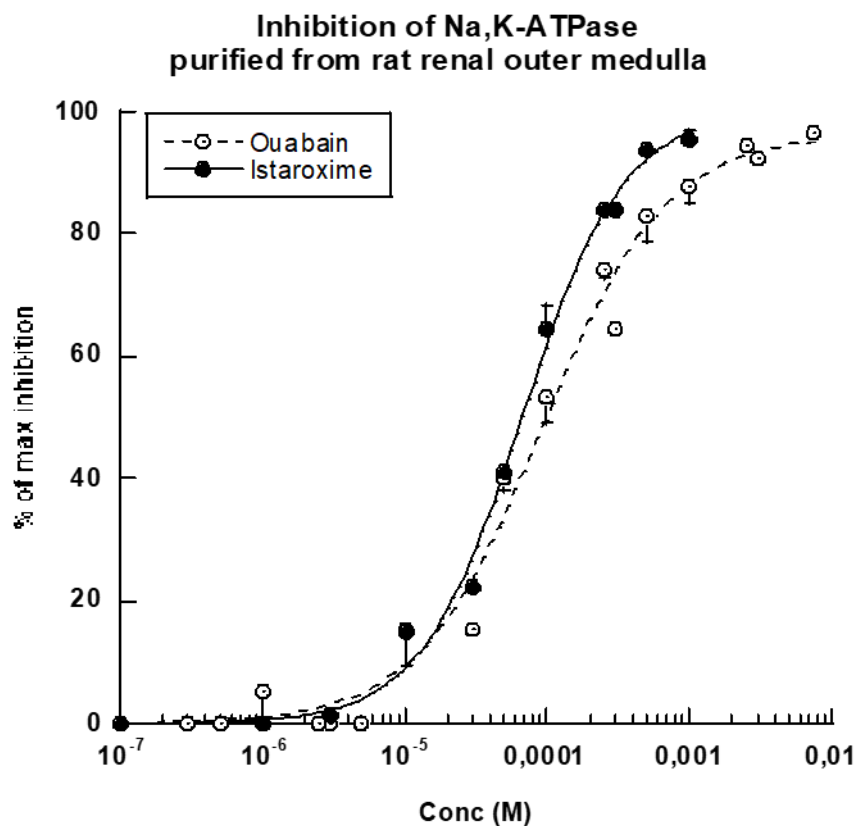


Figure S6. NKA inhibition by istaroxime and ouabain in purified rat kidneys. Concentration-response curves for NKA blockade by istaroxime (N=2) and ouabain (N=3) in purified rat kidneys. NKA activity was assayed *in vitro* by measuring the release of ^{32}P -ATP. The concentration causing 50% inhibition of the NKA activity (IC_{50}) was calculated by using a logistic function and was, respectively, $55 \pm 19 \mu M$ for istaroxime and $96 \pm 26 \mu M$ for ouabain.

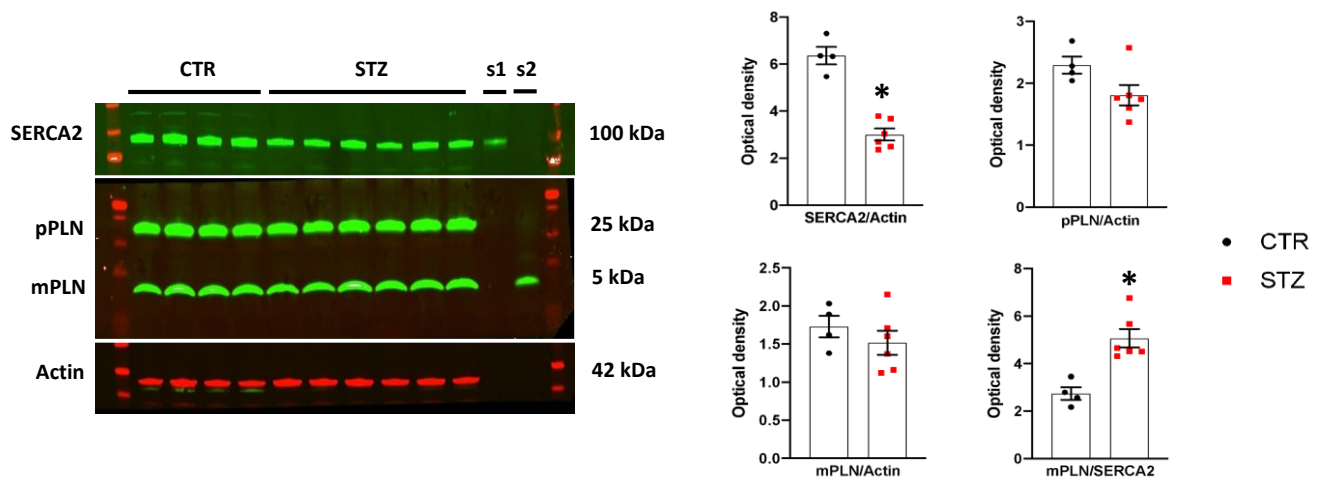


Figure S7. Protein expression levels of SERCA2 and PLN in LV myocytes from CTR and STZ rats. Representative Western blot for SERCA2, monomeric (m) and pentameric (p) PLN in CTR and STZ LV myocytes. Densitometric analysis in arbitrary units is shown on the right. CTR N=4, STZ N=6. * $p < 0.05$ vs CTR (unpaired t -test).

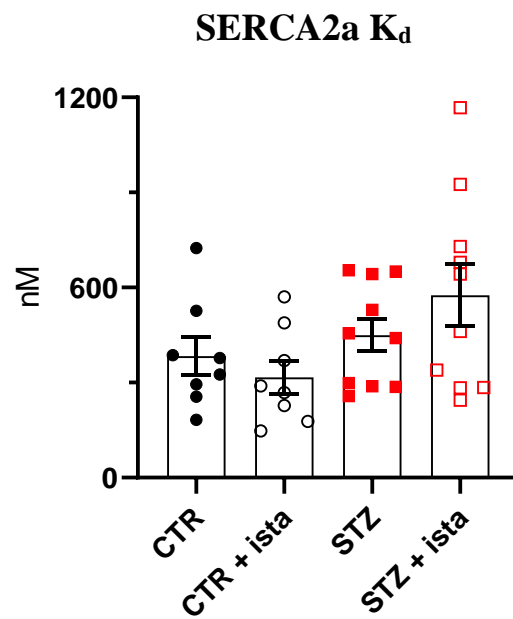


Figure S8. Effects of STZ and istaroxime on SERCA2a Ca^{2+} affinity (K_d) in LV homogenates. The kinetic parameter was estimated by fitting the Ca^{2+} activation curves through a logistic function (see main text Fig 1). CTR N=8, STZ N=10 (with and w/o istaroxime).

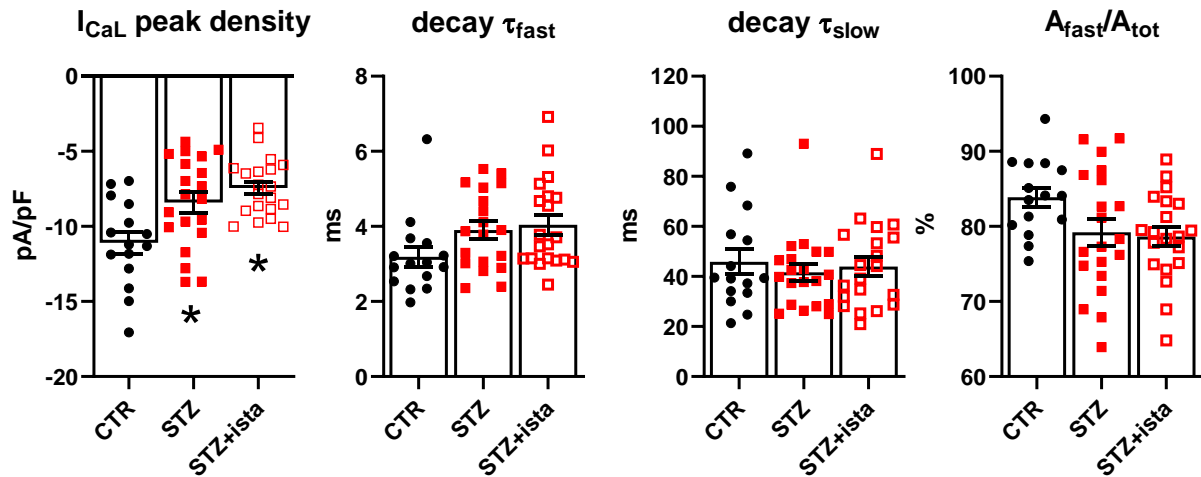


Figure S9. Effects of STZ (with and w/o istaroxime) on nifedipine-sensitive current (I_{CaL}) at 0 mV. Peak I_{CaL} density (pA/pF) and inactivation kinetic components obtained interpolating I_{CaL} decay with a bi-exponential function. Statistics of decay time constants (τ_{fast} and τ_{slow}) and contribution of the fast component to the current decay (A_{fast}/A_{tot}) are shown. CTR N=3, n=15), STZ N=6 (w/o istaroxime n=20, with istaroxime n=20). * $p < 0.05$ vs CTR (one-way ANOVA plus Tukey's multiple comparison).

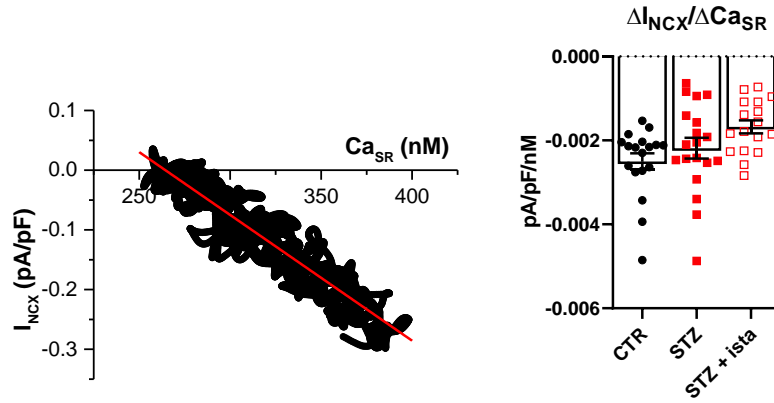


Figure S10. Linear correlation between NCX current (I_{NCX}) and Ca_{SR} (caffeine induced Ca_T) during the final third of the caffeine-induced Ca_T ; average results of the $\Delta I_{NCX} / \Delta Ca_{SR}$ slope on the right (CTR N=3, n=18), STZ N=6 (w/o istaroxime n=19, with istaroxime n=17). See Fig 4B of the main text.

Supplementary methods

Echocardiography

Eight weeks after vehicle/STZ injection, rats were submitted to a transthoracic echocardiographic and Doppler evaluation, performed under urethane (1.25 g/kg i.p.) anesthesia, (M9 Mindray Echographer equipped with a 10 MHz probe, P10-4s Transducer, Mindray, China).

Two-dimensionally guided M-mode recordings were used to obtain short-axis measurements of left ventricular end-diastolic diameter (LVEDD), left ventricular end-systolic diameter (LVESD), posterior wall thickness in diastole (PWTd) and interventricular septum thickness in diastole (IVSTd) according to the American Society of Echocardiography guidelines. Fractional shortening was calculated as $FS = (LVEDD - LVESD)/LVEDD$.

Mitral inflow was measured by pulsed Doppler at the tips of mitral leaflets from an apical 4-chamber view to obtain early and late filling velocities (E, A), and deceleration time (DT) of early filling velocity. The deceleration slope was calculated as the ratio E/DT. The mitral deceleration index was calculated as the ratio DT/E.

Tissue Doppler Imaging (TDI) was evaluated from the apical 4 chamber view to record mitral annular movements, i.e., peak myocardial systolic (s'), and early and late diastolic velocity (e' and a').

End diastolic volume (EDV) and end systolic volume (ESV) were calculated from the diameters using the Teicholz formula. Ejection fraction, expressed as a percentage (EF%), was calculated by the formula: $(EDV-ESV)/EDV*100$.

Heart homogenate preparations

Rats were sacrificed at 9 weeks after STZ injection. Left ventricle (LV) tissues from CTR and STZ rats were rapidly excised, frozen in liquid nitrogen and stored at -80°C . Tissues were homogenized (1g/4ml buffer) in a medium containing 300 mM sucrose, 50 mM K-phosphate, pH 7, 10 mM NaF, 0.3 mM PMSF, 0.5 mM DTT and centrifuged at 35,000g for 30 min. The final pellet was suspended in the same medium and stored in aliquots at -80°C until use.

Protein concentration was determined by Lowry assay² using bovine serum albumin as standard, and molecular purity was checked using SDS-polyacrylamide gel electrophoresis.

Kidney and LV tissues preparations for NKA activity measurements

Renal outer medulla and LV from CTR rats were dissected and suspended (1g/10 ml) in a sucrose-histidine solution containing 250 mM sucrose, 30 mM histidine and 5 mM EDTA, pH 7.2 and homogenized. The homogenate was centrifuged at 6,000 g for 15 min, the supernatant was decanted

and centrifuged at 48,000 g for 30 min. The corresponding pellet contained tissue microsomes. LV microsomes were utilized directly for NKA activity measurements. Conversely, kidney microsomes were further purified on a sucrose gradient. The pellet was suspended in the sucrose-histidine buffer and incubated for 20 min with a sodium-dodecyl-sulphate (SDS) solution, dissolved in a gradient buffer containing 25 mM imidazole and 1 mM EDTA, pH 7.5. The sample was layered on the top of a sucrose discontinuous gradient (10, 15 and 29.4%) and centrifuged at 60,000 g for 115 min. The final pellet was suspended in the gradient buffer.

SERCA2a and NKA activity measurement

SERCA2a activity was measured *in vitro* as ^{32}P -ATP hydrolysis at different Ca^{2+} concentrations (100-3000 nM) as previously described³. The heart homogenate (30 μg) was pre-incubated for 5 minutes at 4°C in 80 μL of a solution containing (mM): 100 KCl, 5 MgCl_2 , 20 Tris, 5 NaN_3 , 0.001 A23187, 0.001 Ruthenium red, at pH 7.4. After pre-incubation, 20 μL of a 5 mM Tris-ATP solution containing 50 nCi of ^{32}P -ATP (0.5-3 Ci/mmol, Perkin Elmer) were added. After 15 min at 37°C, the ATP hydrolysis was stopped by acidification with 100 μL ice-cold perchloric acid 20% v/v. ^{32}P -phosphate was separated by centrifugation with activated charcoal (Norit A, SERVA) and the radioactivity was measured by liquid scintillation counting in a beta counter (Microbeta Trilux, Perkin Elmer). SERCA2a-dependent activity was identified as the portion of total hydrolytic activity inhibited by 10 μM Cyclopiazonic Acid (CPA). Ca^{2+} concentration-response curves were fitted by using a logistic function to estimate SERCA2a Ca^{2+} affinity ($K_d \text{Ca}^{2+}$) and V_{max} .

NKA activity was assayed *in vitro* by measuring the release of ^{32}P -ATP, as previously described⁴. Increasing concentrations of the standard ouabain, or istaroxime, were incubated with 0.3 μg of purified rat kidney enzyme or 20 μg of LV microsomes for 10 min at 37°C in 120 μL final volume of a medium, containing 140 mM NaCl, 3 mM MgCl_2 , 50 mM Hepes-Tris, 3 mM ATP, pH 7.5. Then, 10 μL of incubation solution containing 10 mM KCl and 20 nCi of ^{32}P -ATP (3-10 Ci/mmol) were added, the reaction continued for 15 min at 37°C and was stopped by acidification with 20% v/v ice-cold perchloric acid. ^{32}P was separated by centrifugation with activated Charcoal (Norit A, Serva) and the radioactivity was measured. The inhibitory activity was expressed as percent of the control samples carried out in the absence of ouabain or tested compound. The concentration of compound causing 50% inhibition of the NKA activity (IC_{50}) was calculated by using a logistic function.

Western blot analysis

Samples of LV homogenates or isolated LV myocytes were separated by SDS-polyacrylamide gel electrophoresis (4-12% Bis-Tris Criterion BIO-RAD gels), blotted for 1h and incubated overnight at 4°C with specific primary antibodies, followed by 1h incubation with specific secondary antibodies,

labelled with fluorescent markers (Alexa Fluor or IRDye) and quantified by Odyssey Infrared Imaging System (LI-COR).

Antibodies: polyclonal anti-SERCA2 (N-19; Santa Cruz Biotechnology); monoclonal anti-PLN (2D12, Abcam); polyclonal anti-phospho-Ser¹⁶-PLN (Upstate Millipore); polyclonal anti-phospho-Thr¹⁷-PLN (Santa Cruz); polyclonal anti-Collagen type 1 (Chemicon); polyclonal anti-MMP9 (Abcam); polyclonal anti-actin (Sigma).

Ventricular myocytes preparation

Male Sprague Dawley LV ventricular myocytes were isolated by using a retrograde coronary perfusion method previously published⁵ with minor modifications. Rod-shaped, Ca²⁺-tolerant myocytes were used within 12 h from dissociation.

Myocyte dimensions and T-tubules (TT) analysis

Sarcolemmal membranes were stained by incubating isolated LV myocytes with 20 µmol/L di-3-ANEPPDHQ (Life Technologies, Carlsbad, United States)⁵ dissolved in high K⁺ solution (in mmol/L: 40 KCl, 3 MgCl₂, 70 KOH, 20 KH₂PO₄, 0.5 EGTA, 50 L-Glutamic acid, 20 Taurine, 10 HEPES, 10 Glucose, pH 7.4) for 10 min at room temperature. The excitation-contraction uncoupler blebbistatin (17 µmol/L) was added to inhibit cell motion. Cells were then washed before confocal analysis. Images (1024 x 1024 pixels) were collected with Nikon A1R laser-scanning confocal microscopy equipped with a 60x oil-immersion objective; photomultiplier gain and offset were maintained constant throughout each measurement.

Myocyte were stacked (optical sectioning 1.26 µm) to evaluate cell areas over the entire cell thickness; mean cell area was then evaluated. Cell length, defined as the longest length parallel to the longitudinal axis of the myocyte, was measured in the central section of the cell; cell volume was estimated as mean cell area * cell thickness; the myocyte cross-sectional area (CSA) was estimated from the cell volume/cell length ratio.

TT organization and periodicity was evaluated by a method based on Fast Fourier Transform on 8-bit grayscale images by using TTorg plugin (Fiji)⁶. TT images (1024 x 1024 pixels, 50 µm * 50 µm) were collected with Nikon A1R laser-scanning confocal microscopy. The peak amplitude in the Fourier spectrum of the image at the TT frequency (called TT power) and the TT power spectrum profile of each cell were collected.

Patch clamp measurements

LV myocytes were clamped in the whole-cell configuration (Axopatch 200-A, Axon Instruments Inc., Union City, CA). During measurements, myocytes were superfused at 2 ml/min with Tyrode's solution containing 154 mM NaCl, 4 mM KCl, 2 mM CaCl₂, 1 mM MgCl₂, 5 mM HEPES/NaOH, and 5.5 mM D-glucose, adjusted to pH 7.35. A thermostated manifold, allowing for fast (electronically timed) solution switch, was used for cell superfusion. All measurements were performed at 35 ± 0.5°C. The pipette solution contained 110 mM K⁺-aspartate, 23 mM KCl, 0.2 mM CaCl₂ (calculated free-Ca²⁺=10⁻⁷ M), 3 mM MgCl₂, 5 mM HEPES-KOH, 0.5 mM EGTA-KOH, 0.4 mM GTP-Na⁺ salt, 5 mM ATP-Na⁺ salt, and 5 mM creatine phosphate Na⁺ salt, pH 7.3. Membrane capacitance and series resistance were measured in every cell but left uncompensated. Current signals were filtered at 2 KHz and digitized at 5 KHz (Axon Digidata 1200). Trace acquisition and analysis was controlled by dedicated software (Axon pClamp 8.0).

Na⁺/K⁺ pump current (I_{NKA}) recordings

I_{NKA} was measured as the holding current recorded at -40 mV in the presence of Ni²⁺ (5 mM), nifedipine (5 μM), Ba²⁺ (1 mM) and 4-aminopyridine (2 mM) to minimize contamination by changes in Na⁺/Ca²⁺ exchanger, Ca²⁺ and K⁺ currents, respectively. Tetraethylammonium-Cl (20 mM) and EGTA (5 mM) were added to the pipette solution and intracellular K⁺ was replaced by Cs⁺. To optimize the recording conditions, I_{NKA} was enhanced by increasing intracellular Na⁺ (10 mM) and extracellular K⁺ (5.4 mM). In each cell, the current was recorded at steady state during exposure to increasing concentrations of the drug under test and, finally, to a saturating concentration of ouabain (1 mM). All drugs were dissolved in dimethyl sulfoxide (DMSO). Control and test solutions contained maximum 1:200 DMSO. Because I_{NKA} inhibition was expressed as percentage of ouabain effect, the latter was used as the asymptote for the estimation of IC₅₀ values whenever possible.

A subset of cells was incubated with the Na⁺ indicator Ion NaTRIUM Green-2 AM (5 μM, Abcam) to evaluate changes in intracellular Na⁺ (Na⁺_i) together with changes in membrane current (see below).

Intracellular Na⁺ (Na⁺_i) dynamics

Na⁺_i was monitored in I-clamp condition under physiological condition (Tyrode solution) and in V-clamp condition under modified Tyrode's solution suitable to measure I_{NKA} at the same time (see above). Myocytes were incubated for 30 min with the Na⁺ indicator Ion NaTRIUM Green-2 AM (5 μM, Abcam) and then washed for 15 min to allow dye de-esterification. Dye emission was collected through a 535 nm band pass filter, converted to voltage, low-pass filtered (100 Hz) and digitized at 2 kHz after further low-pass digital filtering (FFT, 50 Hz).

Intracellular Ca²⁺ (Ca²⁺_i) dynamics

Myocytes were incubated in Tyrode solution for 30 min with the membrane-permeant form of the dye, Fluo4-AM (10 μmol/L), and then washed for 15 min to allow dye de-esterification. Fluo4 emission was collected through a 535 nm band pass filter, converted to voltage, low-pass filtered (100 Hz) and digitized at 2 kHz after further low-pass digital filtering (FFT, 50 Hz).

After subtraction of background luminescence, a reference fluorescence (F₀) value was used for signal normalization (F/F₀) (see below for details). Whenever possible, fluorescence was calibrated in nmol/L by estimating in each cell the maximal fluorescence (F_{max}) by increasing at the end of the experiment the intracellular Ca²⁺ concentration through a gentle patch damage. Fluorescence was converted to [Ca]_f according to Eq. S1:

$$[Ca]_f = F * K_d / (F_{max} - F) \quad (\text{Eq. S1})$$

assuming a dye Ca²⁺ dissociation constant (K_d) = 400 nmol/L.

Ca²⁺_i dynamics in field stimulated cells

Ca²⁺_i dynamics were measured in Fluo4-loaded field-stimulated (2 Hz) cardiomyocytes superfused with Tyrode's solution. To highlight the ability of SR to uptake Ca²⁺ at resting (SERCA function) a post-rest potentiation protocol was applied (Fig S1). Briefly, voltage-induced Ca²⁺ transients (Ca_T) were evoked at 2 Hz and steady state Ca_T (ssCa_T) were interrupted by increasing resting pauses (1-5-10-20 s). The amplitude of 1st Ca_T evoked following each resting pause was then normalized to the amplitude of the pre-pause ssCa_T to evaluate SR Ca²⁺ compartmentalization during rest intervals. ssCa_T was evaluated in terms of diastolic Ca²⁺ (Ca_D) and Ca_T amplitude. The SR Ca²⁺ content (Ca_{SR}) was estimated at steady-state by applying an electronically timed 10 mM caffeine pulse. SR Ca²⁺ fractional release (FR) was obtained as the ratio between voltage-induced Ca_T and caffeine-induced Ca_T (Ca_{SR}) amplitude. Moreover, Ca_T decay kinetic was estimated by measuring decay t_{0.5}. Furthermore, after SR Ca²⁺ depletion by caffeine, cells were de novo stimulated and Ca_D values during the reloading process were monitored. Resting Ca²⁺ following SR depletion was used as reference fluorescence (F₀) for signal normalization (F/F₀).

Spontaneous Ca²⁺ release (SCR) events were evaluated in each group at resting and during diastole. A fluorescence increase > 3SD the resting fluorescence was considered a SCR.

Ca²⁺_i dynamics in patch-clamped cells

Firstly, action potential (AP)-clamp experiments were performed (at 2 Hz) to evaluate changes in Ca_T amplitude and Ca_{SR} strictly dependent on AP durations (APDs) only. To this end two AP waveforms

were used as command signals in V-clamp condition and both were applied to the same cell: a “short AP” and a “long AP”, representative of the CTR and STZ group in terms of AP characteristics respectively. Ca_{SR} was estimated as usual at steady state by caffeine superfusion and it was quantified by integrating inward NCX current (I_{NCX}) elicited during caffeine superfusion at -80 mV. At the end of the experiment, F_{max} was estimated in each cell by gentle patch damage to convert fluorescence signals in free Ca^{2+} (Ca_f).

Thus, to highlight direct effects on Ca^{2+}_i handling not depending on electrical activity modifications, Ca^{2+}_i dynamics were also evaluated in voltage-clamped cells by standard V-clamp protocols. $BaCl_2$ (1 mM) and 4-aminopyridine (2 mM) were added to Tyrode’s solution to block K^+ channels. Transmembrane current and cytosolic Ca^{2+} were simultaneously recorded during a train of depolarizing (100 ms) pulses to 0 mV (0.25 Hz) from a holding potential of -40 mV. At steady state condition, an electronically timed 10 mM caffeine pulse was applied at the same cycle length to estimate Ca_{SR} . Fluorescence signal was converted to Ca_f (see above) by measuring F_{max} in each cell; Ca_T amplitude, Ca_{SR} and fractional release (FR) were evaluated. Ca_{SR} was estimated by integrating I_{NCX} elicited by caffeine and by measuring the amplitude of caffeine-induced Ca_T , obtaining similar results. Data from caffeine-induced Ca_T are reported in Fig 4B. The slope of the I_{NCX}/Ca_{SR} relationship during the final third of the caffeine-induced Ca_T was used to estimate NCX ‘conductance’. Ca^{2+} influx through L-type Ca^{2+} channel (Ca_L) was evaluated integrating the nifedipine (10 μ M)-sensitive current during the activation pulse at the peak of the evoked Ca_T and then converted to nmol of Ca^{2+} . Accordingly, the excitation-release (ER) gain was calculated as the ratio between the fraction of nmol of Ca^{2+} released by SR and nmol of Ca^{2+} entered in the cell (Ca_T amplitude- Ca_L)/ Ca_L). I_{CaL} inactivation kinetic was evaluated interpolating current decay with a bi-exponential function; fast and slow decay time constant (τ_{fast} and τ_{slow}) and the proportion of fast or slow component to the total decay (e.g. A_{fast}/A_{tot}) were estimated.

Finally, to estimate SR uptake function in the absence of NCX and NKA function, SR reloading protocol was applied in V-clamped cells by removing Na^+ from both sides of the sarcolemma as previously described^{1,7,8}. Cells were incubated in a Na^+/Ca^{2+} -free solution (replaced by equimolar Li^+ and 1 mM EGTA) added with 4-aminopyridine (2 mM) to block K^+ channels. The pipette solution was Na^+ -free (Na^+ salts were replaced by Mg^{2+} or Tris salts). The protocol consisted in emptying the SR by a caffeine pulse (with 154 mM Na^+ to allow Ca^{2+} extrusion through NCX) and then progressively refilling it by voltage steps to 0 mV activating Ca^{2+} influx through I_{CaL} in the presence of 1 mM Ca^{2+} (Fig S2). Kinetics of SR Ca^{2+} reloading was evaluated in terms of rate of Ca_T amplitude and ER gain enhancement during the loading process. ER gain in this protocol setting was simply evaluated as the ratio between Ca_T amplitude and Ca_L influx at the peak of Ca_T within each pulse.

Moreover, we considered the time constant of Ca_T decay (τ_{decay}) reflecting Ca^{2+} transport rate across the SR membrane, a functional index of SERCA2a activity.

Ca²⁺ sparks rate and characteristics

Spontaneous unitary Ca^{2+} release events (Ca^{2+} sparks) were recorded at room temperature in Fluo 4-AM (10 μM) loaded myocytes at resting condition. Tyrode's bath solution contained 1 mM CaCl_2 . Images were acquired at x60 magnification in line-scan mode (*xt*) at 0.5 kHz by confocal Nikon A1R microscope. Each cell was scanned along a longitudinal line and #10 *xt* frames (512 pxls x 512 pxls) were acquired. Non-cell fluorescence was acquired too to allow background fluorescence subtraction. Confocal setting parameters were kept constant throughout all experimental groups to permit group comparison analysis. Images were analyzed by SparkMaster plugin (Fiji) software⁹. Automatic spark detection threshold (criteria) was imposed to 3.8. Only in focus Ca^{2+} sparks (amplitude > 0.3) were considered to quantify their characteristics. In particular, the following spark parameters were measured: frequency (N of events/s/100 μm), amplitude ($\Delta F/F_0$), full width at half-maximal amplitude (FWHM, μm), full duration at half-maximal amplitude (FDHM, ms), full width (FW, μm) and full duration (FD, ms), time to peak (ttp, ms) and decay time constant (τ , ms). Spark mass (spark amplitude*1.206* FWHM³) was also calculated as index of Ca^{2+} spark volume¹⁰.

Compounds

Stock Fluo4-AM (1 mM in DMSO) and Ion NaTRIUM Green-2 (1 mM in DMSO) solutions were diluted in Tyrode's solution. Istaroxime was dissolved in DMSO at 10-100 mM and then diluted to get final concentrations from 100 nM to 1 mM. The final DMSO did not exceed 0.1% (if it is not different specify). Istaroxime was synthesized at SciAnda (Changshu) Pharmaceuticals Ltd, Jiangsu (China). Fluo4-AM from ThermoFisher Scientific-Life Technologies Italia, Ion NaTRIUM Green-2 from Abcam and all other chemicals from Merck (Darmstadt, Germany).

References

1. Rocchetti M, Besana A, Mostacciolo G, Micheletti R, Ferrari P, Sarkozi S, Szegedi C, Jona I, Zaza A. Modulation of sarcoplasmic reticulum function by Na⁺/K⁺ + pump inhibitors with different toxicity: Digoxin and PST2744 [(E,Z)-3-((2-aminoethoxy)imino)androstane-6,17-dione hydrochloride]. *J Pharmacol Exp Ther* 2005;**313**:207–215.
2. Lowry OH, Rosebrough NJ, Farr AL, Randall RJ. Protein measurement with the Folin phenol reagent. *J Biol Chem* 1951;**193**:265–275.

3. Micheletti R, Palazzo F, Barassi P, Giacalone G, Ferrandi M, Schiavone A, Moro B, Parodi O, Ferrari P, Bianchi G. Istaroxime, a Stimulator of Sarcoplasmic Reticulum Calcium Adenosine Triphosphatase Isoform 2a Activity, as a Novel Therapeutic Approach to Heart Failure. *Am J Cardiol* 2007;**99**:24A-32A.
4. Ferrandi M, Tripodi G, Salardi S, Florio M, Modica R, Barassi P, Parenti P, Shainskaya A, Karlish S, Bianchi G, Ferrari P. Renal Na,K-ATPase in genetic hypertension. *Hypertension* 1996;**28**:1018–1025.
5. Rocchetti M, Sala L, Rizzetto R, Irene Staszewsky L, Alemanni M, Zambelli V, Russo I, Barile L, Cornaghi L, Altomare C, Ronchi C, Mostacciuolo G, Lucchetti J, Gobbi M, Latini R, Zaza A. Ranolazine prevents INaL enhancement and blunts myocardial remodelling in a model of pulmonary hypertension. *Cardiovasc Res* 2014;**104**:37–48.
6. Pasqualin C, Gannier F, Malécot CO, Bredeloux P, Maupoil V. Automatic quantitative analysis of t-tubule organization in cardiac myocytes using ImageJ. *Am J Physiol - Cell Physiol* 2015;**308**:C237-45.
7. Rocchetti M, Alemanni M, Mostacciuolo G, Barassi P, Altomare C, Chisci R, Micheletti R, Ferrari P, Zaza A. Modulation of sarcoplasmic reticulum function by PST2744 [Istaroxime; (E,Z)-3-((2-aminoethoxy)imino) androstane-6,17-dione hydrochloride] in a pressure-overload heart failure model. *J Pharmacol Exp Ther* 2008;**326**:957–965.
8. Alemanni M, Rocchetti M, Re D, Zaza A. Role and mechanism of subcellular Ca²⁺ distribution in the action of two inotropic agents with different toxicity. *J Mol Cell Cardiol* 2011;**50**:910–918.
9. Picht E, Zima A V., Blatter LA, Bers DM. SparkMaster: Automated calcium spark analysis with ImageJ. *Am J Physiol - Cell Physiol* 2007;**293**:C1073–C1081.
10. Hollingworth S, Peet J, Chandler WK, Baylor SM. Calcium sparks in intact skeletal muscle fibers of the frog. *J Gen Physiol* 2001;**118**:653–678.